Hindawi Publishing Corporation
Journal of Nanomaterials
Volume 2010, Article ID 512785, 10 pages
doi:10.1155/2010/512785

Research Article

Effect of Postdeposition Heat Treatment on the Crystallinity, Size, and Photocatalytic Activity of TiO_2 Nanoparticles Produced via Chemical Vapour Deposition

Siti Hajar Othman, Suraya Abdul Rashid, Tinia Idaty Mohd Ghazi, and Norhafizah Abdullah

Department of Chemical and Environmental Engineering, Faculty of Engineering, University of Putra, 43400 Serdang, Selangor, Malaysia

Correspondence should be addressed to Suraya Abdul Rashid, suraya@eng.upm.edu.my

Received 7 December 2009; Revised 27 March 2010; Accepted 8 May 2010

Academic Editor: Theodore Tsotsis

Titanium dioxide (TiO_2) nanoparticles were produced using chemical vapour deposition (CVD) at different deposition temperatures (300–700°C). All the samples were heat treated at their respective deposition temperatures and at a fixed temperature of 400°C. A scanning electron microscope (SEM), a transmission electron microscope (TEM), and X-ray diffraction (XRD) were used to characterize the nanoparticles in terms of size and crystallinity. The photocatalytic activity was investigated via degradation of methylene blue under UV light. The effects of post deposition heat treatment are discussed in terms of crystallinity, nanoparticle size as well as photocatalytic activity. Crystallinity was found to have a much larger impact on photocatalytic activity compared to nanoparticle size. Samples having a higher degree of crystallinity were more photocatalytically active despite being relatively larger in size. Surprisingly, the photocatalytic activity of the samples reduced when heat treated at temperatures lower than the deposition temperature despite showing an improvement in crystallinity.

1. Introduction

The most popular choice of photocatalyst is titanium dioxide (TiO_2), and much of the published work on photocatalysis uses this material [1, 2]. TiO_2 is a promising photocatalyst due to its easy availability, low cost, photoactivity, high stability, nontoxicity, hydrophilicity, and high refractive index. TiO_2 can be used for a variety of purposes including self-cleaning surfaces, antibacterial, air purification, and water treatment applications. Lately there has been an increasing amount of research done to enhance the photocatalytic efficiency of TiO_2 for better use of this photocatalyst.

One of the ways to improve the photocatalytic efficiency of TiO_2 is by heat treatment. Generally, heat treatment is a process to remove a volatile fraction or to cause a phase transition in solid materials. Heat treatment of TiO_2 has the advantage of removing organic impurities within the TiO_2 and promotes crystallinity for better photocatalytic efficiency [3]. The impurities within TiO_2 may arise during the synthesis process. For example, carbon impurities within TiO_2 may originate from the organic precursor used during sample preparation. Meanwhile, the crystal structure of TiO_2 is known to exist in a stable phase called rutile and two metastable phases called anatase and brookite. Anatase is irreversibly transformed into rutile upon application of heat. Although the rutile phase has a wide variety of applications, primarily in the pigment industry, the anatase phase with a band gap of 3.2 eV is usually preferred because it has proven to be the most active crystal structure that possesses higher levels of photoactivity compared to the other phases due to its favourable energy band positions and high surface area [2].

To date, many methods have been used to synthesize TiO_2 including pulsed laser deposition [4], diffusion flame reactor [5], water in oil emulsion [6], hydrothermal synthesis [7, 8], and chemical vapour deposition (CVD) [9]. Among them, CVD is a favourable technique to synthesize TiO_2 due to the ease and simplicity of the process. The control

of size distribution and the type of crystal structure of the TiO_2 nanoparticles produced can be easily accomplished by simply controlling the CVD parameters such as deposition temperature and gas flowrate. Moreover, a CVD reactor has the potential to be scaled up to industrial-scale production levels.

To the best of our knowledge, only one work has been undertaken to study the effect of heat treatment temperatures on the properties of TiO_2 produced using CVD. Wang et al. [3] studied the effect of heat treatment temperatures on the crystal structure and photocatalytic activity of TiO_2 film produced using CVD at low deposition temperatures (<350°C). They heat treated the samples at a temperature range of 450 to 850°C for 24 hours and found that the best photocatalytic activity of the TiO_2 film was observed at a deposition temperature of 350°C and a heat treatment temperature of 550°C. Note that they did not study the effect of heat treating TiO_2 at temperatures lower than the deposition temperature.

In this work, CVD was used to produce TiO_2 nanoparticle samples using a wider range of deposition temperatures (300–700°C). The morphology of TiO_2 nanoparticle samples was studied by scanning electron microscope (SEM). To study the effects of postdeposition heat treatment on the properties of the TiO_2 nanoparticles, the samples were then heat treated at their respective deposition temperatures as well as at a fixed temperature of 400°C for one hour. The effect of the heat treatment temperature on the crystallinity, size, and the photocatalytic activity of the samples was studied via X-ray diffraction (XRD), transmission electron microscopy (TEM), and via the degradation of methylene blue under UV light, respectively.

2. Experimental

2.1. Synthesis of TiO_2 Nanoparticles. The CVD setup consists of stainless steel gas flow lines, mass flow controllers, a bubbler, and a quartz tube (52 mm outside diameter (o.d.) and 800 mm long) in a split tube furnace acting as the reactor. The heating zone was 300 mm long. The precursor, titanium (IV) butoxide (TBOT) obtained from Sigma-Aldrich, was used as received, was stored in a stainless steel bubbler located on a hot plate, and maintained at 175°C. The quartz tube was purged by nitrogen (400 mL/min) during the initial heating step towards reaching the desired deposition temperature (between 300 to 700°C). Once the reaction temperature was achieved, the precursor was introduced into the quartz tube using nitrogen as the carrier gas (400 mL/min). TiO_2 nanoparticles would then be thermophoretically deposited inside the quartz tube upon thermal decomposition of the precursor gas. After 3 hours of reaction time, the flow of the precursor gas inside the reactor was stopped by switching off the carrier gas valve, and the reactor was allowed to cool down to room temperature under a 400 mL/min nitrogen flow. The nanoparticles were then collected from the quartz tube wall using a spatula and kept in a small container.

Postdeposition thermal treatment was performed in this study in an open split tube furnace. All the samples were heat treated for 1 hour at 400°C as well as at their respective deposition temperatures.

2.2. Characterization Method. The size and morphology of TiO_2 nanoparticle samples were studied by SEM (LEO 1455 VP) and TEM (Hitachi H7100). The crystalline phase of the TiO_2 nanoparticle samples with and without heat treatment was determined using XRD (Philips X'pert Pro PW3040) with a Cu Kα radiation source ($\lambda = 0.15406$ nm) operated at 40 kV and 30 mA.

2.3. Photocatalytic Study. A simple photocatalytic reactor was used in this study. The photocatalytic study was performed at room temperature. A volume of 400 mL of 6 ppm methylene blue was poured into a 500 mL cylinder which was placed on a magnetic stirrer. An 8 W, 254 nm UV lamp was immersed in the methylene blue. Following this, 0.02 g of TiO_2 nanoparticles were introduced inside the cylinder. The UV light and magnetic stirrer along with an air pump (to supply air for the photocatalytic oxidation reaction) were switched on simultaneously. A volume of 6 mL of suspension was then taken out every minute for the first 10 minutes and then every 5 minutes for the following 50 minutes. A UV-Vis spectrophotometer (Thermo Scientific Helios Alpha) was used to determine the absorbance value at 664 nm (absorbance peak of methylene blue). All experimental runs were repeated 3 times.

Note that the temperature of the suspension was found to increase from 30 to 39°C during the 1-hour period of the experiment. It is generally accepted that increasing the reaction temperature can affect the photocatalytic activity. However, in this case the change in temperature is quite small (<10°C) hence the effect of temperature in our photocatalytic study was expected to be negligible. Kaneco et al. [10] who studied the effect of temperature from 10 to 40°C on the photocatalytic degradation of dibutyl phthalate by TiO_2 found that an appreciable change was not observed in this temperature range.

3. Results and Discussions

3.1. TiO_2 Nanoparticles without Heat Treatment

3.1.1. Crystal Structure. The crystal structure of TiO_2 nanoparticle samples deposited at 300–700°C was examined by XRD as shown in Figure 1. The XRD pattern for the sample deposited at 300°C showed no detectable peaks indicating that the sample was amorphous. Meanwhile, the peaks at 2θ values of 25.3, 37.8, 48.0, 53.8, and 54.9 for the samples deposited at temperatures of 400°C and above correspond to the diffractions of the (1 0 1), (0 0 4), (2 0 0), (1 0 5), and (2 1 1) planes of anatase, respectively [9, 11]. These peaks confirmed that the samples were in the anatase crystal structure. From the XRD data, there were no other detectable peaks to suggest the presence of a rutile crystal structure. This result is consistent with the findings of Zhang et al. [12] that showed only the peak characteristic of the anatase phase in

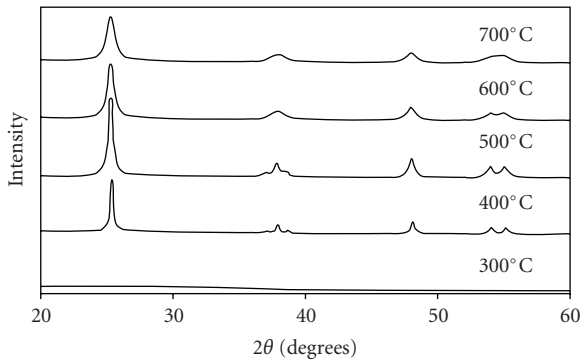

Figure 1: XRD patterns of TiO_2 nanoparticle samples deposited at various deposition temperatures.

their XRD spectra for TiO_2 nanoparticle samples produced using CVD at deposition temperatures of 500°C and 700°C.

It can also be seen from Figure 1 that the peaks of the XRD patterns corresponding to the diffraction of the (1 0 1) plane of anatase become broader at higher temperatures. This observation indicates that the nanoparticle size becomes smaller as the temperature is increased. This observation is also supported by the SEM micrographs shown in Figure 2.

3.1.2. Size and Morphology. Figure 2 compares the SEM micrographs of TiO_2 nanoparticle samples deposited at 400–700°C. The respective size distribution histogram of the nanoparticles in terms of diameter, which were determined using the ImageJ software, is also shown. The histograms were fitted using a Gaussian distribution. The mean nanoparticle diameter and standard deviation are also included. The micrographs show that the nominal diameter of the particles is less than 100 nm and that they appear to be relatively homogeneous and uniform in size except for the sample deposited at 400°C. It can be seen that increasing the deposition temperature has a direct effect on the particle size. There is a trend of decreasing the mean diameter from 76.5 to 24.1 nm when the deposition temperature is increased from 400 to 700°C, which is consistent with the findings of Nakaso et al. [13]. They discovered that at a lower reactor temperature (<800°C), the primary particle size of TiO_2 deposited using a metal organic precursor, in their case titanium tetraisopropoxide (TTIP), decreased with increasing temperature. Moreover, the size distribution histograms in Figure 3 illustrate that the increase in temperature causes an orderly decrease in the size distribution. This finding indicates that a higher deposition temperature generates smaller nanoparticles with a narrower size distribution.

The mean nanoparticle diameter of the samples was also calculated by applying the Debye-Scherrer formula [1] on the anatase (1 0 1) diffraction peaks

$$D = \frac{K\lambda}{\beta \cos\theta}, \quad (1)$$

where D is the mean nanoparticle diameter, K is a constant which is taken as 0.89 for a spherical crystalline shape, λ is the wavelength of the X-ray radiation (Cu $K\alpha = 0.15406$ nm), β is the corrected band broadening at full width at half-maximum (fwhm), and θ is the diffraction angle. The XRD data indicates that there was a significant decrease from 49.6 to 20.7 nm as the deposition temperature increased from 400 to 700°C. Despite the slight deviation in the values calculated using Debye Scherrer formula, especially for lower temperature, the results are consistent with the values obtained from the SEM micrographs.

3.1.3. Thermogravimetry Analysis. Thermogravimetry (TGA) analysis of the synthesized TiO_2 samples was undertaken to determine the minimum heat treatment temperature for total elimination of impurities in the TiO_2 nanoparticles. The TGA result as shown in Figure 3 indicates that a total weight loss of ~6.9% was achieved at 400°C for sample deposited at 700°C. This trend was also observed for all of the other samples (Figure not shown). This finding is supported by Jitputti et al. [14] who in their study found that a heat treatment temperature of 400°C was sufficient for complete removal of the organic substances from synthesized mesoporous TiO_2. García-Serrano et al. [15] also found that elimination of organic components from TiO_2 nanoparticles synthesized using the modified sol-gel method occurred at around 400°C. Therefore, for qualitative purposes, a heat treatment temperature of 400°C was considered adequate for the significant removal of most, if not all, organic impurities within the samples. Note that after the heat treatment process, all of the samples which originally had a slightly greyish tinge (most probably due to carbon) turned to white in colour indicating that the impurities were mostly eliminated. To examine the effect of heat treatment temperatures on the crystal structure, size, and photocatalytic activity of the samples, all the samples were heat treated at both 400°C as well as at their respective deposition temperatures.

3.2. TiO_2 Nanoparticles with Heat Treatment

3.2.1. Crystal Structure. Figures 4(a)–4(e) represent the XRD patterns for all the samples with and without heat treatment for comparison. The figures show that a mere 1-hour heat treatment process has a significant effect on the crystallinity of the TiO_2 nanoparticle samples. From Figure 4(a), it can be seen that the amorphous samples obtained at a deposition temperature of 300°C became anatase when they were heat treated at both 300 and 400°C. Wang et al. [3] had previously reported that amorphous TiO_2 deposited at a low temperature transformed into polycrystalline anatase after being heat treated at a higher temperature. Moreover, Pal et al. [16] found that amorphous samples produced using a modified sol-gel technique became anatase after being heat treated at 400°C thus supporting this finding. It seems that a phase transition from amorphous to anatase occurs at a temperature of less than 300°C.

Figures 4(a)–4(e) also reveal that the peak height of anatase increased with a rise in heat treatment temperature. In general, the anatase peak became higher for all the samples

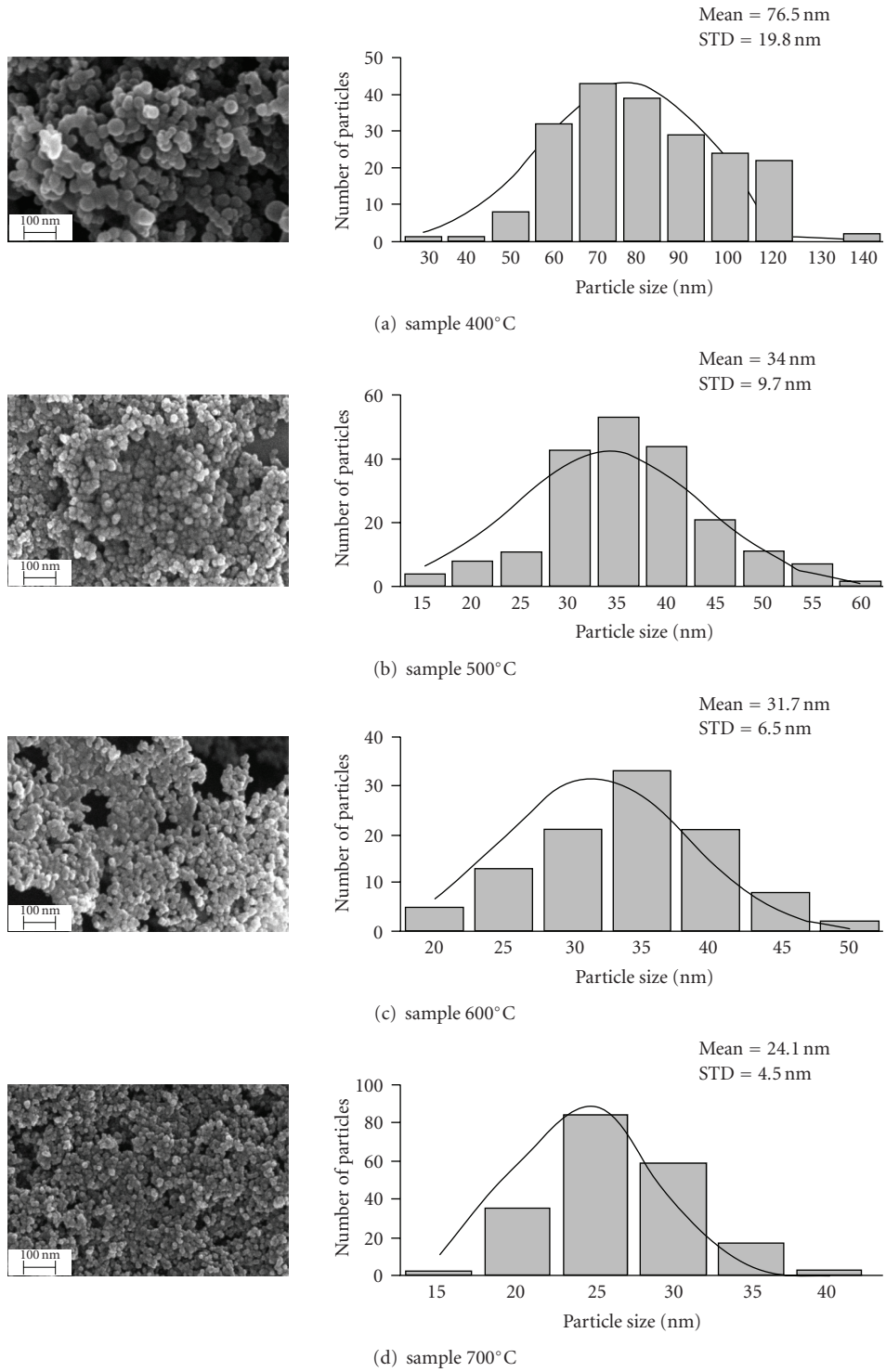

Figure 2: SEM micrographs (left) and respective nanoparticle size distribution histograms (right) for TiO_2 nanoparticle samples deposited by CVD at (a) 400°C, (b) 500°C, (c) 600°C, and (d) 700°C.

that underwent postdeposition heat treatment, but even more so for the higher heat treatment temperatures such as 600 and 700°C. This indicates that a higher heat treatment temperature promotes the formation of the anatase crystal structure. This result is also in agreement with Jitputti et al. [14] who found that an increase in the heat treatment temperature resulted in improved crystallinity of their mesoporous TiO_2 samples prepared by the hydrothermal method.

Figure 4(e) shows new apparent peaks for the sample deposited and treated at 700°C. These new peaks at 2θ values of 27.4, 36.1, 41.2, and 54.3 correspond to the diffractions

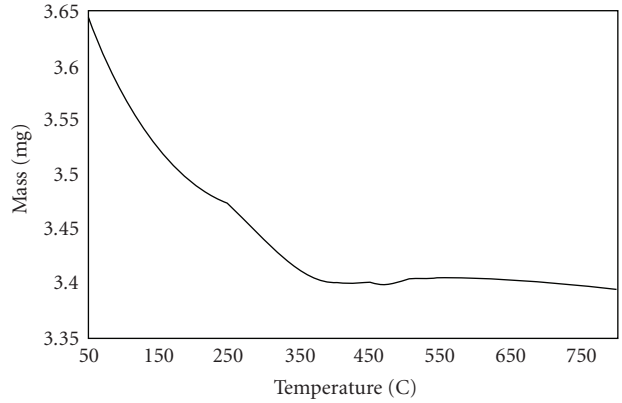

Figure 3: TGA curve of the sample synthesized at 700°C.

of the (1 1 0), (1 0 1), (1 1 1), and (2 1 1) planes of rutile, respectively, [14]. These peaks indicate that the sample has a mixture of anatase and rutile crystal structures. The fractions of anatase and rutile crystal structures were calculated according to the following [2]:

$$f_A = \frac{1}{1 + (1/K)(I_R/I_A)}, \quad K = 0.79, \quad f_A > 0.2, \quad K = 0.68, \quad f_A \leq 0.2, \tag{2}$$

where f_A is the fraction of anatase crystal structure in the samples, I_A and I_R are the X-ray intensities of the anatase (1 0 1) and rutile (1 1 0) diffraction peaks, respectively, and K is a constant. For the samples deposited and heat treated at 700°C, the anatase and rutile fractions were found to be 75 and 25%, respectively. These results suggest that the phase transition from anatase to rutile occurs at a temperature in the range of 600 to 700°C.

Many studies have determined that heat treatment at a higher temperature favours rutile formation. For example, Chhabra et al. [17] found that heat treatment at 1000°C for microemulsion-mediated TiO_2 nanoparticles led to complete rutile transformation. In this current study, a heat treatment temperature of 700°C is sufficiently high enough for partial transition from anatase to rutile. Pal et al. [16] and Hamadanian et al. [18] found that the formation of the rutile phase for TiO_2 nanoparticles began at 650°C which seems to be consistent with the results obtained in this study.

In general, the effect of heat treatment on the crystallinity and phase transition of TiO_2 nanoparticles does not depend a great deal on their synthesis technique. Irrespective of the synthesis technique used, heat treatment will always enhance crystallinity and at a certain temperature, phase transition will occur. García-Serrano et al. [15] have studied the effect of heat treatment on the crystallization and phase transition of undoped and Ag-doped TiO_2 nanoparticles under different atmospheres, and they came to the same conclusion; heat treatment at a higher temperature enhances crystallinity and favours rutile formation. However, according to Gennari and Pasquevich [19], there is no specific temperature that can be assigned to the phase transition. The phase transition temperature relies on parameters such as synthesis technique, reaction atmosphere, impurity content, particle size, and the oxygen vacancy concentrations within the TiO_2 lattice.

Furthermore, it is also interesting to compare the crystallinity of the samples deposited at different temperatures after being heat treated at the same temperature of 400°C. The comparison using XRD spectra is given in Figure 4(f). The results show that the sample deposited at 400°C and heat treated at 400°C had the highest peak intensity and hence a higher degree of crystallinity. It can be concluded from Figure 4 that samples heat treated at a temperature equal or greater than the deposition temperature have a higher degree of crystallinity compared to samples heat treated at a temperature lower than the deposition temperature.

3.2.2. Size and Morphology. TEM analysis was carried out to determine the effects of post-deposition heat treatment on the size and morphology of TiO_2 nanoparticles. Figure 5 compares the TEM micrographs before and after heat treatment of the samples deposited at 700°C. The size distribution histogram of the nanoparticles is also shown. The micrographs illustrate that the nominal diameter of the particles is less than 50 nm and that they appear to be fairly homogeneous and equal in size.

It can be seen that post-deposition heat treatment temperature has a direct effect on the particle size whereby the mean particle diameter increases from 18.5 to 22.4 nm after undergoing heat treatment at 400°C. The size increment becomes even more pronounced at a higher heat treatment temperature whereby the mean particle diameter becomes 32.9 nm after undergoing heat treatment at 700°C. This trend is also observed for all the other samples (Figure not shown). In addition, Figure 5 shows that the increase in heat treatment temperature results in an increase in size distribution. This finding implies that a higher heat treatment temperature leads to the formation of larger nanoparticles with a wider size distribution.

The increase in particle size is possibly due to sintering effects consistent with the findings of other researchers. Jitputti et al. [14] also found that increasing the heat treatment temperature from 400 to 600°C resulted in an increase in the particle size of their mesoporous TiO_2 samples. Hamadanian et al. [18] who produced TiO_2 nanoparticles using a modified sol-gel method and Yu et al. [20] who produced thin films using the liquid phase deposition method both observed similar results of increasing particle size with an increase in heat treatment temperature. Conversely, Pal et al. [16] found the opposite result. The size of TiO_2 particles synthesized using glycolated precursors reduced from 432 nm to about 230 nm as the heat treatment temperature was increased to 850°C. Perhaps it can be deduced that sintering effects become effective for relatively small nanoparticles (<100 nm) with not much volume to lose from the removal of organic impurities.

3.3. Photocatalytic Activity. The photocatalytic activity of the samples was evaluated via the degradation of methylene blue

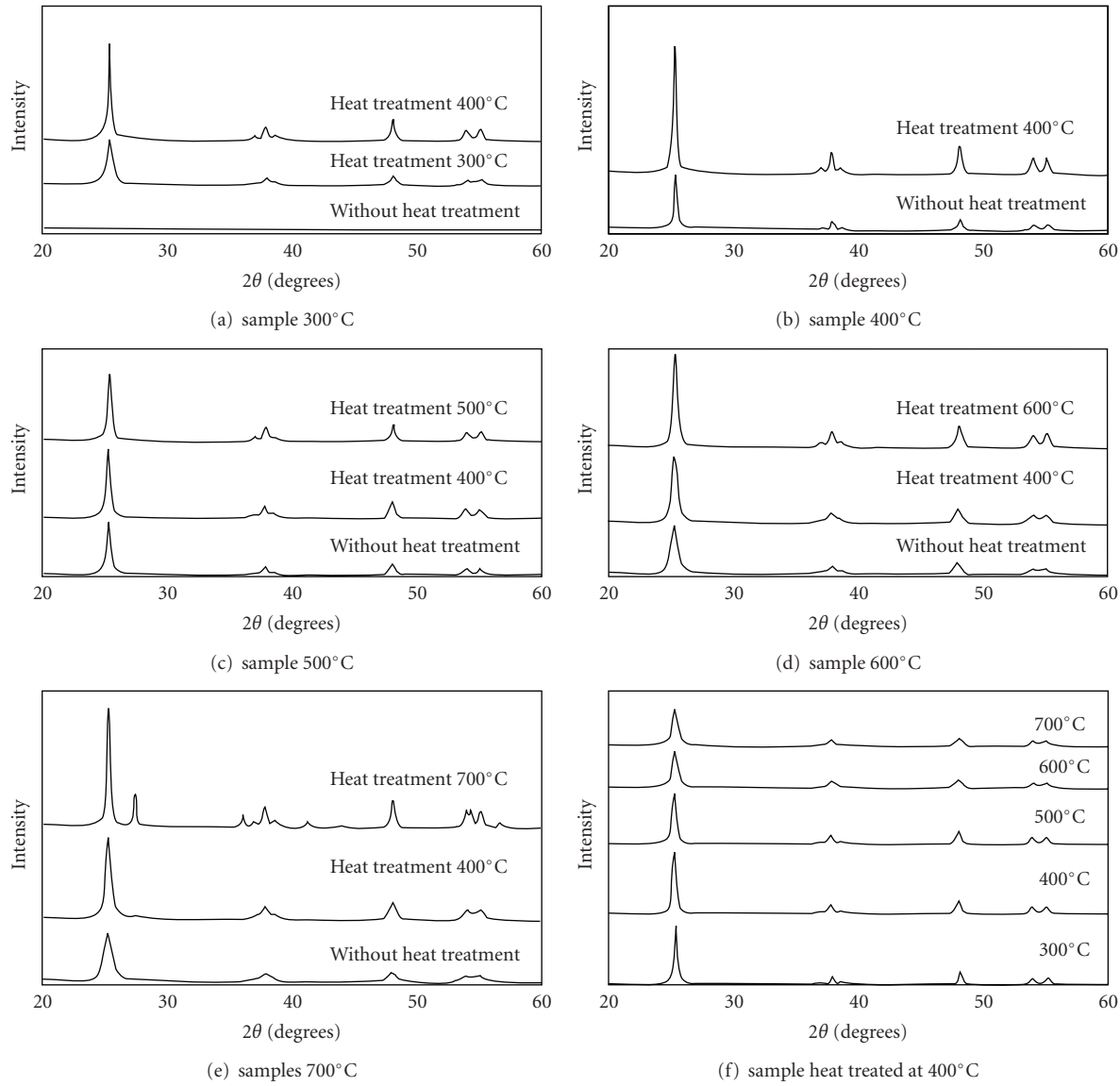

Figure 4: XRD patterns for the TiO_2 nanoparticle samples deposited at different deposition temperatures with and without heat treatment—(a) 300°C, (b) 400°C, (c) 500°C, (d) 600°C, (e) 700°C, and (f) XRD patterns for all samples deposited at different temperatures, heat treated at 400°C.

aqueous solution over a period of 1 hour. The degradation of methylene blue occurred very fast and was almost complete after only 20 minutes of reaction time. The photocatalytic activity for all the samples was quantitatively evaluated for the first 20 minutes by calculating the respective pseudo-first order rate constants (k) according to:

$$\ln\left(\frac{C_o}{C}\right) = kt, \tag{3}$$

where C_o and C are, respectively, the initial concentration and the reaction concentration of methylene blue at time t. Figures 6(a)–6(e) show the plots of $\ln(C_0/C)$ against time for all the samples. Meanwhile, Figure 6(f) compares the photocatalytic activity of samples deposited at different temperatures and heat treated at the same temperature of 400°C. The fitted linear trend lines with respective R^2 values are also shown.

It can be seen from Figure 6 that all of the samples are able to decompose methylene blue as indicated by the decrease in the methylene blue solution concentration throughout the period of the photocatalytic study except for the sample deposited at 300°C. This is due to the amorphous nature of this sample. The slight decrease in methylene blue concentration for the amorphous sample is likely due to the interaction of the methylene blue with OH- which originated from water [21].

For clarity purposes, the rate constants obtained from the slope of the fitted linear trend lines are tabulated in Table 1. The rate constant represents the photocatalytic activity of the TiO_2 nanoparticle samples. The higher the rate constant,

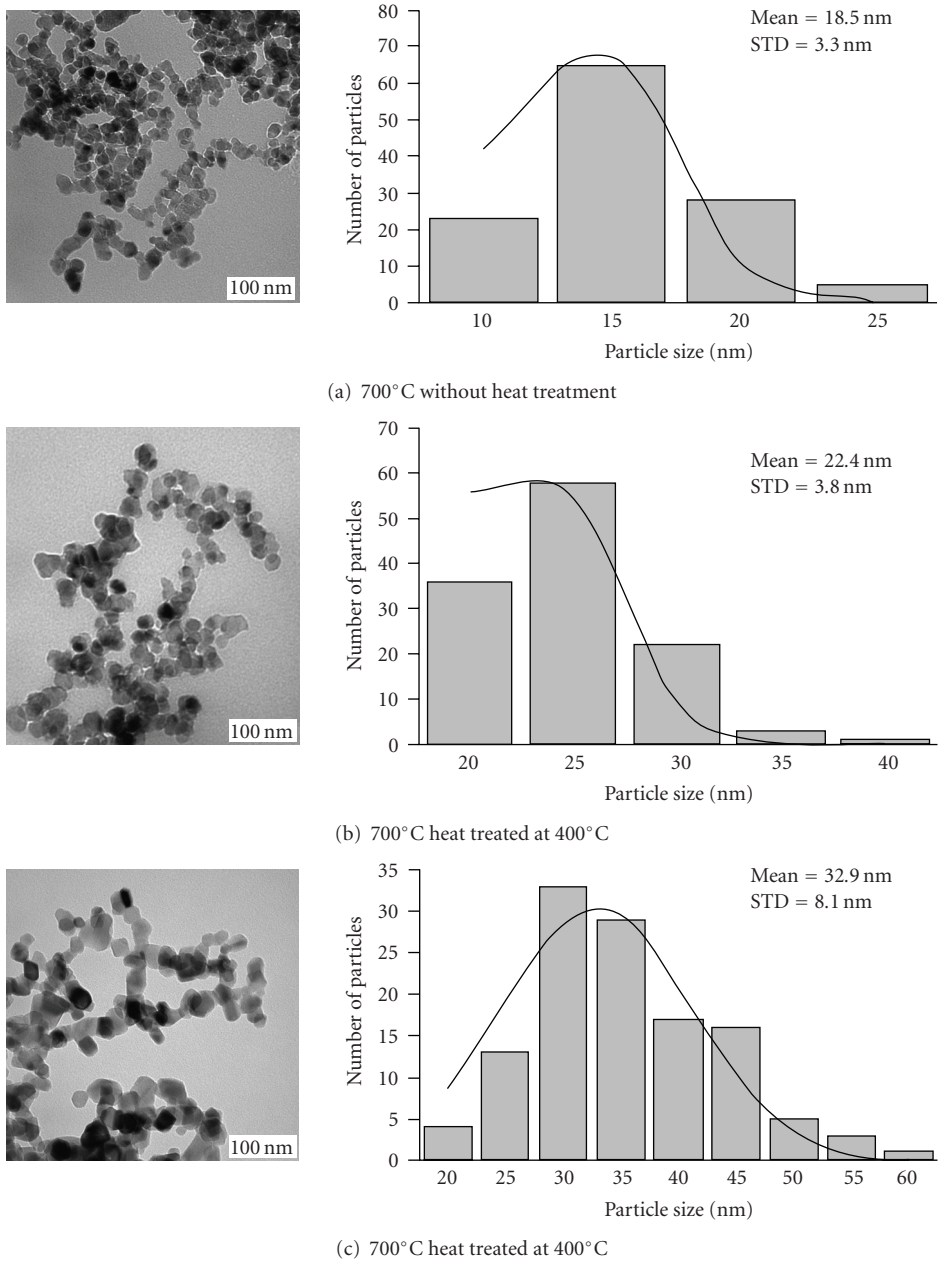

Figure 5: TEM micrographs (left) and respective nanoparticle size distribution histograms (right) of TiO_2 nanoparticle samples deposited by MOCVD at (a) 700°C, (b) 700°C heat treated at 400°C, and (c) 700°C heat treated at 700°C.

the faster the degradation of methylene blue hence the better the photocatalytic activity of the samples.

Three salient observations regarding the photocatalytic activity of the samples can be deduced from Table 1 in terms of nanoparticle size, crystallinity, and choice of heat treatment temperature. Firstly, for samples without heat treatment, it can be seen that the photocatalytic activity increases as the size of the nanoparticles decreases, as expected. The rate constant for samples A, D, F, I, and L increased from 0.28 to 5.89 h^{-1}. The improvement in photocatalytic activity is most probably due to the increase in surface area for photocatalysis to occur as the nanoparticles become smaller [22].

Secondly, the effects of crystallinity on the photocatalytic activity can be seen when comparing samples that have undergone heat treatment at 400°C, that is, samples C, E, G, J, and M (their mean diameters were 49.6, 31.0, 27.6, 25.2, and 22.5 nm, resp., as calculated using (1)). Samples C and E have higher rate constant values compared to samples G, J, and M. This indicates that samples heat treated at temperatures higher than or equal to the deposition temperature have better photocatalytic activity. This observation can be attributed to the higher degree of crystallinity which has been discussed previously in Figure 4(f).

Also note that despite samples C, E, and G being relatively larger in size compared to samples J and M, they had

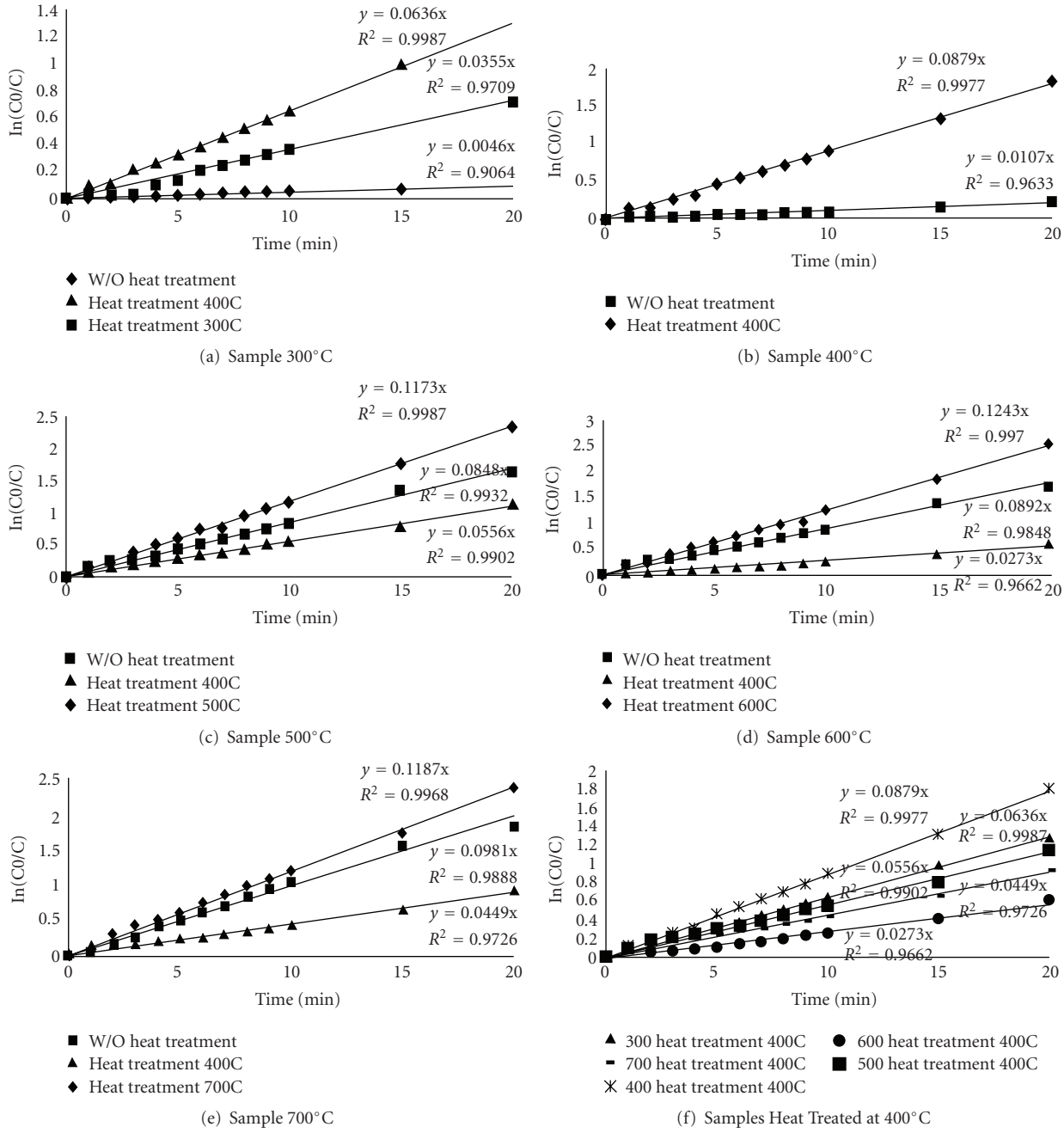

Figure 6: Photocataytic activity for TiO_2 nanoparticle samples deposited at different deposition temperatures with and without heat treatment—(a) 300°C, (b) 400°C, (c) 500°C, (d) 600°C, (e) 700°C, and (f) Photocatalytic activity of samples deposited at different deposition temperatures and heat treated at 400°C. Graphs fitted with linear trend line from which the rate constants were determined.

better photocatalytic activity. This can also be clearly seen in Figure 6(f). On the other hand, sample M, being smaller in size, had a better photocatalytic activity than sample J. However, their moderate degree of crystallinity was in fact almost similar. Therefore, it can be deduced that although both crystallinity and nanoparticle size are two important factors that influence the photocatalytic activity of heat treated TiO_2 samples, crystallinity plays a more significant role compared to size. However, for relatively moderate degrees of crystallinity (as is also the case for samples without heat treatment), nanoparticle size becomes important.

Thirdly, it can be seen that the effectiveness of the heat treatment process is very much dependent on the deposition temperature of the TiO_2 nanoparticle sample. Postdeposition heat treatment of samples at temperatures higher than or equal to the deposition temperature (samples C, E, H, K, and N) leads to an enhancement in photocatalytic activity. This result is consistent with the finding of Wang et al. [3]

Table 1: The rate constant values for the TiO_2 nanoparticle samples with and without heat treatment and the mean particle diameter determined from SEM for samples without heat treatment.

Sample	Deposition Temperature (°C)	Heat Treatment Temperature (°C)	Rate Constant, k (h^{-1})	Mean Particle Diameter from SEM (nm)
A	300	—	0.28	
B	300	300	2.13	
C	300	400	3.82	
D	400	—	0.64	76.5
E	400	400	5.27	
F	500	—	5.09	34.0
G	500	400	3.34	
H	500	500	7.04	
I	600	—	5.35	31.7
J	600	400	1.64	
K	600	600	7.46	
L	700	—	5.89	24.1
M	700	400	2.70	
N	700	700	7.12	

that showed an improvement in photocatalytic conversion of toluene as the samples were heat treated at a temperature greater than the deposition temperature provided that no rutile crystal structure exists. It is generally accepted that heat treatment enhances the photocatalytic activity of TiO_2 by reducing organic impurities and promoting crystallinity and that the effect becomes more pronounced as the heat treatment temperature is increased [3, 14]. The XRD results shown previously in Figures 4(a)–4(e) also support this behaviour.

However, it is not entirely clear as to why heat treatment of samples at a temperature lower than the deposition temperature causes a significant decrease in photocatalytic activity, especially since the XRD results shown previously in Figures 4(a)–4(e) also indicate an improvement in crystallinity. Sintering effects have been known to decrease the photocatalytic activity of samples due to the decrease in surface area. However, Figures 5(b) and 5(c) show that sintering effects are more significant at a higher heat treatment temperature. More detailed studies are being carried out to investigate these findings. Nonetheless, it can be concluded that for TiO_2 samples produced using the CVD method, the choice of heat treatment temperature should be made in view of the deposition temperature.

It was also observed that the photocatalytic activity of sample N was slightly less than sample K. According to Nishimoto et al. [2], the anatase crystal structure has a better photocatalytic activity than the rutile form. Since some of the anatase crystal structure transformed to rutile for sample N, the photocatalytic activity of the samples may have been affected. On the other hand, other studies have shown that optimal photocatalytic activity is obtained with a mixture of anatase and a small percentage of rutile [1]. Therefore, the lowering of photocatalytic activity at the relatively high heat treatment temperature of 700°C could have also been due to sintering effects which decreases the surface area of the sample. Yu et al. [20] observed similar results in their work for TiO_2 thin films. Hamadanian et al. [18] attributed the decrease in photoactivity of TiO_2 nanoparticles synthesized from sol-gel method heat treated at 500–700°C to the sintering phenomena. For this particular study, sample K which was deposited and heat treated at 600°C possessed the highest photocatalytic activity.

4. Conclusions

TiO_2 nanoparticles were successfully synthesized using CVD at deposition temperatures of 300–700°C. The samples were all anatase in nature with relatively moderate levels of crystallinity except for the sample obtained at 300°C which was amorphous. SEM micrographs showed that increasing the deposition temperature led to smaller nanoparticles with a narrower size distribution. As expected, the photocatalytic activity of the samples increased as nanoparticle size decreased most probably due to the availability of a larger surface area for photocatalysis to occur.

The synthesized samples were then heat treated at both the respective deposition temperatures as well as at a fixed temperature of 400°C. XRD results disclosed that heat treatment promotes crystallinity, with samples achieving higher degrees of crystallinity at higher heat treatment temperatures. Furthermore, sintering phenomena were also seen for heat treated samples.

The effects of postdeposition heat treatment on the photocatalytic activity of the TiO_2 nanoparticles were described in terms of crystallinity, nanoparticle size as well as the choice of heat treatment temperature. Crystallinity was found to have a much larger impact on photocatalytic activity compared to nanoparticle size (surface area) whereby samples having a higher degree of crystallinity were more photocatalytically active despite being relatively larger in size.

It was found that the samples heat treated at temperatures higher than or equal to the deposition temperature had improved photocatalytic activity. Surprisingly, the photocatalytic activity of samples became worse when heat treated at temperatures lower than the deposition temperature despite having an improvement in crystallinity. Therefore, it was deduced that for TiO_2 nanoparticles produced using CVD, the choice of heat treatment temperature should be made in view of the deposition temperature.

Acknowledgment

This work was financially supported by Fundamental Research Grant Scheme, University Putra Malaysia (Grant no. 5523426).

References

[1] M. Yan, F. Chen, J. Zhang, and M. Anpo, "Preparation of controllable crystalline titania and study on the photocatalytic properties," *Journal of Physical Chemistry B*, vol. 109, no. 18, pp. 8673–8678, 2005.

[2] S. Nishimoto, B. Ohtani, H. Kajiwara, and T. Kagiya, "Correlation of the crystal structure of titanium dioxide prepared from titanium tetra-2-propoxide with the photocatalytic activity for redox reactions in aqueous propan-2-ol and silver salt solutions," *Journal of the Chemical Society, Faraday Transactions*, vol. 81, no. 1, pp. 61–68, 1985.

[3] K.-H. Wang, Y.-H. Hsieh, T.-T. Lin, and C.-Y. Chang, "Effects of temperature on the properties of TiO_2 photocatalysts prepared by the chemical vapor deposition (CVD) method," *Reaction Kinetics and Catalysis Letters*, vol. 95, no. 1, pp. 39–46, 2008.

[4] R. Paily, A. DasGupta, N. DasGupta, et al., "Pulsed laser deposition of TiO_2 for MOS gate dielectric," *Applied Surface Science*, vol. 187, no. 3-4, pp. 297–304, 2002.

[5] H. D. Jang and S.-K. Kim, "Controlled synthesis of titanium dioxide nanoparticles in a modified diffusion flame reactor," *Materials Research Bulletin*, vol. 36, no. 3-4, pp. 627–637, 2001.

[6] Y. Mori, Y. Okastu, and Y. Tsujimoto, "Titanium dioxide nanoparticles produced in water-in-oil emulsion," *Journal of Nanoparticle Research*, vol. 3, no. 2-3, pp. 219–225, 2001.

[7] M. Wu, J. Long, A. Huang, Y. Luo, S. Feng, and R. Xu, "Microemulsion-mediated hydrothermal synthesis and characterization of nanosize rutile and anatase particles," *Langmuir*, vol. 15, no. 26, pp. 8822–8825, 1999.

[8] M. Andersson, A. Kiselev, L. Österlund, and A. E. C. Palmqvist, "Microemulsion-mediated room-temperature synthesis of high-surface-area rutile and its photocatalytic performance," *Journal of Physical Chemistry C*, vol. 111, no. 18, pp. 6789–6797, 2007.

[9] W. Li, S. Ismat Shah, C.-P. Huang, O. Jung, and C. Ni, "Metallorganic chemical vapor deposition and characterization of TiO_2 nanoparticles," *Materials Science and Engineering B*, vol. 96, no. 3, pp. 247–253, 2002.

[10] S. Kaneco, H. Katsumata, T. Suzuki, and K. Ohta, "Titanium dioxide mediated photocatalytic degradation of dibutyl phthalate in aqueous solution-kinetics, mineralization and reaction mechanism," *Chemical Engineering Journal*, vol. 125, no. 1, pp. 59–66, 2006.

[11] X. Zhang, M. Zhou, and L. Lei, "Co-deposition of photocatalytic Fe doped TiO_2 coatings by MOCVD," *Catalysis Communications*, vol. 7, no. 7, pp. 427–431, 2006.

[12] X. Zhang, M. Zhou, L. Lei, and S. Xu, "Synthesis of TiO_2 supported on activated carbon by MOCVD: operation parameters study," *Journal of Zhejiang University: Science*, vol. 5, no. 12, pp. 1548–1553, 2004.

[13] K. Nakaso, K. Okuyama, M. Shimada, and S. E. Pratsinis, "Effect of reaction temperature on CVD-made TiO_2 primary particle diameter," *Chemical Engineering Science*, vol. 58, no. 15, pp. 3327–3335, 2003.

[14] J. Jitputti, S. Pavasupree, Y. Suzuki, and S. Yoshikawa, "Synthesis and photocatalytic activity for water-splitting reaction of nanocrystalline mesoporous titania prepared by hydrothermal method," *Journal of Solid State Chemistry*, vol. 180, no. 5, pp. 1743–1749, 2007.

[15] J. García-Serrano, E. Gómez-Hernández, M. Ocampo-Fernández, and U. Pal, "Effect of Ag doping on the crystallization and phase transition of TiO_2 nanoparticles," *Current Applied Physics*, vol. 9, no. 5, pp. 1097–1105, 2009.

[16] M. Pal, J. G. Serrano, P. Santiago, and U. Pal, "Size-controlled synthesis of spherical TiO_2 nanoparticles: morphology, crystallization, and phase transition," *Journal of Physical Chemistry C*, vol. 111, no. 1, pp. 96–102, 2007.

[17] V. Chhabra, V. Pillai, B. K. Mishra, A. Morrone, and D. O. Shah, "Synthesis, characterization, and properties of microemulsion-mediated nanophase TiO_2 particles," *Langmuir*, vol. 11, no. 9, pp. 3307–3311, 1995.

[18] M. Hamadanian, A. Reisi-Vanani, and A. Majedi, "Preparation and characterization of S-doped TiO_2 nanoparticles, effect of calcination temperature and evaluation of photocatalytic activity," *Materials Chemistry and Physics*, vol. 116, no. 2-3, pp. 376–382, 2009.

[19] F. C. Gennari and D. M. Pasquevich, "Kinetics of the anatase-rutile transformation in TiO_2 in the presence of Fe_2O_3," *Journal of Materials Science*, vol. 33, no. 6, pp. 1571–1578, 1998.

[20] J.-G. Yu, H.-G. Yu, B. Cheng, X.-J. Zhao, J. C. Yu, and W.-K. Ho, "The effect of calcination temperature on the surface microstructure and photocatalytic activity of TiO_2 thin films prepared by liquid phase deposition," *Journal of Physical Chemistry B*, vol. 107, no. 50, pp. 13871–13879, 2003.

[21] M. Panizza, A. Barbucci, R. Ricotti, and G. Cerisola, "Electrochemical degradation of methylene blue," *Separation and Purification Technology*, vol. 54, no. 3, pp. 382–387, 2007.

[22] H. D. Jang, S.-K. Kim, and S.-J. Kim, "Effect of particle size and phase composition of titanium dioxide nanoparticles on the photocatalytic properties," *Journal of Nanoparticle Research*, vol. 3, no. 2-3, pp. 141–147, 2001.